

Axisymmetric bending of a circular plate with symmetrically varying mechanical properties under a concentrated force

Krzysztof Magnucki*, Włodzimierz Stawecki^a and Jerzy Lewinski^b

Łukasiewicz Research Network - Institute of Rail Vehicles TABOR,
ul. Warszawska 181, 61-055 Poznań, Poland

(Received October 17, 2019, Revised February 14, 2020, Accepted February 17, 2020)

Abstract. The subject of the paper is a circular plate with symmetrically thickness-wise varying mechanical properties. The plate is simply supported and carries a concentrated force located in its centre. The axisymmetric bending problem of the plate with consideration of the shear effect is analytically and numerically studied. A nonlinear function of deformation of the straight line normal to the plate neutral surface is assumed. Two differential equations of equilibrium based on the principle of stationary potential energy are obtained. The system of equations is analytically solved and the maximum deflections and shear coefficients for example plates are derived. Moreover, the maximum deflections of the plates are calculated numerically (FEM), for comparison with the analytical results.

Keywords: circular plate; bending; functionally graded materials; shear effect; nonlinear theory

1. Introduction

The thin-walled plates make part of the structures and, therefore, are the subject of the contemporary studies. Timoshenko and Woinowsky-Krieger (1959) and Ventsel and Krauthammer (2001) presented detailed grounds of the theory, analysis and applications of thin plates and shells, taking into account the papers and monographs of the 20th century. Zingoni (2002) studied the problem of two conical shells intersecting each other. The results verified by finite element analysis, were useful for evaluation of the stresses and deformations in double-cone pressure vessels. Magnucki *et al.* (2002) dealt with stress concentration in a cylindrical pressure vessel with ellipsoidal heads subjected to internal pressure. It was shown that the stress concentration scale depends on the ratio of thicknesses of both adjacent parts of the shells and on relative convexity of the ellipsoidal head. Zingoni (2002) investigated stress distribution in the egg-shaped sludge digesters composed of two joined paraboloidal shells. A single governing parameter was formulated that simplifies designing the concrete sludge-digester shells. Krivoschapko (2007) delivered a review of the achievements in the design and construction of thin-walled axisymmetric ellipsoidal shells. The author analyzed many references presenting the results of experimental investigations of the stress-strain state, buckling, and natural and forced vibrations of these structures. Zingoni *et al.* (2015) considered bending of an

elliptic toroidal shell. An approximate solution was formulated that enables accurate simulation of the edge effects arising due to the loads and geometric discontinuities in the equatorial plane of elliptic toroids. Zingoni *et al.* (2018) presented a linear-elastic theoretical formulation allowing to determine the state of stress in large thin-walled vessels composed of multi-segmented spherical shells. The results of finite element computation confirmed accurateness and effectiveness of the method. Sowiński and Magnucki (2008) examined possible reduction of the edge effect in three nonstandard dished heads of a cylindrical pressure vessel. The authors considered several shapes of the head meridian. The problem was solved analytically and positively verified by numerical (FEM) approach.

The works devoted to non-homogeneous structures have been initiated in the mid of the 20th century. These structures are permanently improved and complemented by the concept of functionally graded materials until to-day. Ferreira *et al.* (2003) dealt with the composite laminated plates using the third-order Reddy's theory. The authors developed a new meshless method in order to discretize the structure. It enabled to predict the plate behaviour with high accuracy. Zenkour (2006) presented the problem of a rectangular plate under the transverse uniform load, using the author's own earlier developed generalized shear deformation theory. The functionally graded properties of the plate material have been adopted. The effects of transversal shear deformation, geometric ratios and volume distribution on the plate behaviour have been investigated. Magnucka-Blandzi (2008) focused on buckling and deflection of a circular porous plate loaded with radial uniform compression and pressure. Properties of the plate material varied in thickness direction. The principle of stationarity of the total potential energy allowed to derive a system of differential equations governing the plate

*Corresponding author, Professor

E-mail: krzysztof.magnucki@tabor.com.pl

^a Ph.D.

^b DSc.

stability. Its solution enabled to determine the plate critical load and deflection. Saidi *et al.* (2009) used the third-order shear deformation plate theory to study bending and buckling of functionally graded circular plates. The results of maximum displacement and critical buckling load achieved in this approach for various ceramic-metal ratios were compared to those obtained with the use of other plate theories. Sahraee and Saidi (2009) studied axisymmetric bending of functionally graded circular plates under uniform transverse load. The analytical model was formulated using fourth-order shear deformation plate theory. Maximum deflection and shear stress were calculated. Shen (2009) analyzed the plates and shells made of functionally graded materials. The problems of modelling of these structures was presented. The higher order shear deformation theory of the plates was used in order to derive the nonlinear equations governing the plate behaviour. The author considered bending, nonlinear vibration and postbuckling behaviour of shear deformable plates. Reddy (2010) used the constitutive relations of Eringen and the idea of von Kármán nonlinear strains with a view to formulate anew the classical and shear deformation beam and plate theories. The equilibrium equations and a finite element model was developed, allowing for assessing the effect of the geometric nonlinearity and the constitutive relations on bending response of the considered structures. Yun *et al.* (2010) investigated the problem of axisymmetric bending of transversely isotropic and functionally graded circular plates under a transverse load, expanded in the Fourier–Bessel series. The direct displacement method was used for the purpose. In some cases the analytical solutions were workable. The numerical examples verified the proposed method. Gunes and Aydin (2010) studied the impact bending of functionally graded circular plates composed of ceramic and metal layers. The influence of the layer number, the through-thickness variation gradient of the mechanical properties, the impactor velocity and plate radius on the circular plate response was investigated. The failure strains were determined with a view to locate the damage regions of the layers. Debowski *et al.* (2010) dealt with a rectangular plate made of isotropic metal foam the mechanical properties of which varied in the thickness direction. The Hamilton's principle allowed to derive a system of partial differential equations of the plate motion. Solution of the equations was compared to FEM numerical results. Reddy and Berry (2012) formulated an original theory of axisymmetric bending of circular plates, based on microstructure of the material and the classical and first-order shear deformation theories. Mechanical properties of the material varied according to power-law. The effect of the nonlinearity, power-law index, and microstructural relationships on the response of axisymmetric analysis of circular plates was assessed. Jha *et al.* (2013) delivered a review of the research dedicated to functionally graded plates, with consideration of the publications dated after 1997. The authors dealt with the works devoted to deformation, stress, vibration and stability problems of these structures. The review was aimed at presentation of the studies and applications in the field of *functionally* graded plates. Maturi *et al.* (2014) analyzed the static and

dynamic (free vibration) behaviour of sandwich plates, the facing and core materials of which differ one from the other. A new layerwise theory was developed, using the radial basis functions, that enabled precise calculation of the transverse normal and shear deformations as well as the stresses. Several examples of the composite sandwich plates were tested and elaborated. Jabbari *et al.* (2014) studied buckling of a circular plate made of porous material, the mechanical properties of which vary across the thickness. The Love-Kirchhoff hypothesis was applied with a view to consider geometrical nonlinearities of the plate. The prebuckling and critical forces were calculated. The results were compared to those of homogeneous circular plates. Mojahedin *et al.* (2016) used the higher order shear deformation theory with a view to analyze buckling of circular plates made of saturated porous materials. The plate was considered as geometrically perfect, with its mechanical properties varying in thickness direction. The equations governing the plate behaviour were derived based on the Sanders non-linear strain–displacement relationship. The results, i.e. the prebuckling and critical forces, were compared to the ones reported in the literature. Wu and Liu (2016) used the Reissner mixed variational theorem in order to develop a method of analysis of the circular plates made of functionally graded material. The quality of this method was assessed by comparing the solutions with the accurate ones available in the literature. Feyzi and Khorshidvand (2017) studied axisymmetric post-buckling behavior of a circular plate made of porous material saturated with fluid, subjected to uniformly distributed radial compression. The authors investigated the effect of the size and distribution of the pores, fluid compressibility, thickness variations and boundary conditions on the plate post-buckling behaviour. The results were compared to those obtained by other researchers. Beni and Dehkordi (2018) used the Carrera unified formulation converted to the polar coordinates in order to analyze the behaviour of a circular sandwich plate. The functionally graded material, the core of the plate was made of, was considered as a mixture of ceramics and metal. Its mechanical properties varied according to a power law in the direction of thickness. The results were compared to those available in the literature as well as the ones obtained with the generalized zig-zag theory, showing a proof of high accuracy of the new approach. Wu and Yu (2018) analyzed two-directional functionally graded circular plates using the Reissner's mixed variational theorem. The solutions were perfectly compatible with those obtained using the 3D analytical approach and two-dimensional plate theories presented in the literature. Magnucka-Blandzi *et al.* (2018) dealt with a thin-walled three-layer circular plate, composed of two facings and a metal foam core of varying mechanical properties. A mathematical model considering the shear effect was developed, that was aimed at solving the plate global buckling problem. The principle of stationary total potential energy enabled to derive the equations of equilibrium. Numerical verification with finite element method indicated correctness of the method. Magnucki (2018) delivered an analytical study of buckling of a cylindrical panel. The mechanical properties of the panel varied in the thickness

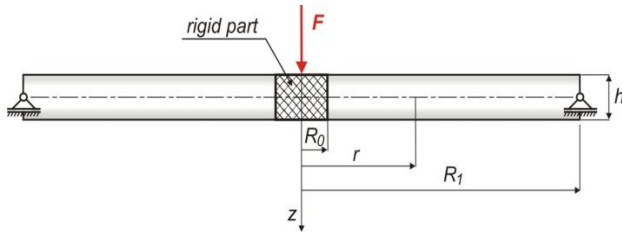


Fig. 1 Scheme of the circular plate with the load

direction. Based on the principle of stationary total potential energy the equations governing the panel behaviour were derived. Assumption of a nonlinear hypothesis of deformation of a straight line perpendicular to the panel neutral surface during buckling led to the analytical solutions providing the critical loads. Magnucki *et al.* (2019) considered a rectangular plate with its mechanical properties varying symmetrically in the thickness direction. A nonlinear hypothesis of deformation of the straight line normal to neutral surface of the plate was adopted which allowed to determine the field of the displacements. The Hamilton's principle served as a basis for derivation of the equations of motion. Their solution allowed to calculate the critical loads and natural frequencies of several exemplary plates. The results were verified with finite element method.

The subject of the studies is a simply supported circular plate of radius R_1 and thickness h with a rigid central part of radius R_0 . The plate is subjected to a concentrated force F (Fig. 1). The problem is studied in linear-elastic range.

The concentrated force applied directly to a thin-walled structure would easily damage it. Therefore, the force must be spread over a certain area that must be reinforced in order to transfer the force. Hence, the considered plate is provided with a rigid central part to which the force is applied, that complies with practice.

2. Analytical model of the plate

The symmetrical thickness-wise variation of mechanical properties of the circular plate is similar to the case presented by Magnucki (2018) and Magnucki *et al.* (2019). In these papers the variation of Young's modulus is presented by trigonometric functions. Taking into account the paper Magnucki and Lewiński (2019) the Young's modulus of the circular plate is assumed to vary according to the following power function

$$E(\zeta) = E_1 f_e(\zeta) \quad (1)$$

where the dimensionless function

$$f_e(\zeta) = e_0 + (1 - e_0)(6\zeta^2 - 32\zeta^6)^{k_e} \quad (2)$$

and: $\zeta = z/h$ – dimensionless coordinate, $e_0 = E_0/E_1$ – dimensionless parameter, E_0, E_1 – Young's moduli for $\zeta=0$ and $\zeta=\pm 1/2$, k_e – exponent – real positive number ($1 \leq k_e$).

The nonlinear theory-hypothesis of deformation of a straight line normal to middle surface of the plate is assumed. The graphical illustration of the hypothesis is

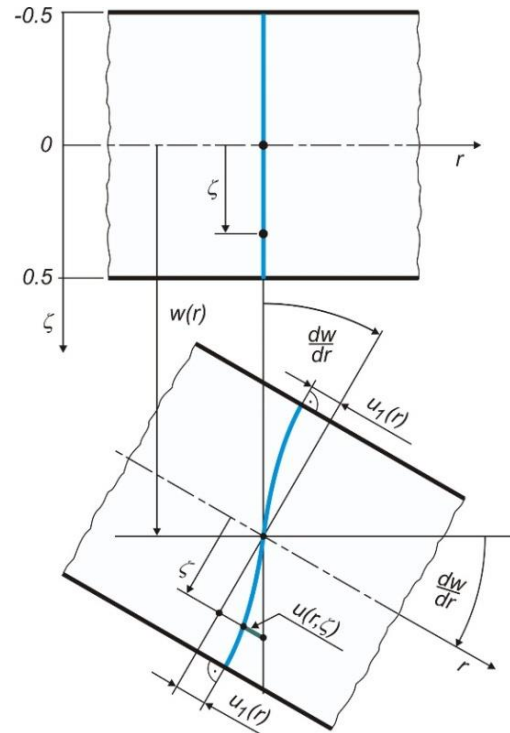


Fig. 2 The scheme of the straight normal line deformation after bending

shown in Fig. 2. The straight normal line before bending transforms into a curve after bending. This curve is perpendicular to the upper and lower surfaces of the plate and, in consequence, the shear stresses at these surfaces are zero. This hypothesis takes into consideration the shear effect in the circular plate.

The longitudinal displacement in accordance with Fig. 2 is as follows

$$u(r, \zeta) = -h \left[\zeta \frac{dw}{dr} - f_d(\zeta) \psi(r) \right] \quad (3)$$

where: $w(r)$ – deflection, $\psi(r) = u_1(r)/h$ – dimensionless displacement function.

The nonlinear hypothesis formulated by Magnucki (2018) and Magnucki and Lewiński (2019) is generalized to a new original function taking the following form

$$f_d(\zeta) = (3\zeta - 4\zeta^3)^7 + \sum_{j=1}^5 \beta_j \left[1 - (3\zeta - 4\zeta^3)^{7-j} \right] (3\zeta - 4\zeta^3) \quad (4)$$

where: β_j – dimensionless coefficients ($j=1, 3, 5$).

The first derivative of the function is as follows

$$\frac{df_d}{d\zeta} = 3 \left(7(3\zeta - 4\zeta^3)^6 + \sum_{j=1}^5 \beta_j \left[1 - 7(3\zeta - 4\zeta^3)^{7-j} \right] \times (3\zeta - 4\zeta^3)^{j-1} (1 - 4\zeta^2) \right) \quad (5)$$

The strains

$$\begin{aligned}\varepsilon_r(r, \zeta) &= \frac{\partial u}{\partial r} = -h \left[\zeta \frac{d^2 w}{dr^2} - f_d(\zeta) \frac{d\psi}{dr} \right] \\ \varepsilon_\varphi(r, \zeta) &= \frac{u(r, \zeta)}{r} = -h \left[\zeta \frac{dw}{rdr} - f_d(\zeta) \frac{\psi(r)}{r} \right] \quad (6) \\ \gamma_{rz}(r, \zeta) &= \frac{\partial u}{h d\zeta} + \frac{dw}{dr} = \frac{df_d}{d\zeta} \psi(r)\end{aligned}$$

where r, φ - the polar coordinates.

The transverse shear strain $\gamma_{rz}(r, \zeta)$ along the thickness is a convex function (Magnucki (2018)), hence

$$0 \leq \left. \frac{d^2 f_d}{d\zeta^2} \right|_{-1/2} \quad \text{and} \quad \left. \frac{d^2 f_d}{d\zeta^2} \right|_{1/2} \leq 0, \quad (7)$$

from which the condition for dimensionless coefficients values of the function (5) is in the following form

$$3\beta_1 + 2\beta_3 + \beta_5 \leq \frac{7}{2} \quad (8)$$

The stresses in accordance with the Hooke's law

$$\begin{aligned}\sigma_r(r, \zeta) &= \frac{E_1}{1-\nu^2} [\varepsilon_r(r, \zeta) + \nu \varepsilon_\varphi(r, \zeta)] f_e(\zeta) \\ \sigma_\varphi(r, \zeta) &= \frac{E_1}{1-\nu^2} [\varepsilon_\varphi(r, \zeta) + \nu \varepsilon_r(r, \zeta)] f_e(\zeta) \quad (9) \\ \tau_{rz}(r, \zeta) &= \frac{E_1}{2(1+\nu)} \gamma_{rz}(r, \zeta) f_e(\zeta)\end{aligned}$$

Taking into account the paper (Magnucki 2018) a constant value of the Poisson's ratio for the material of the plate is assumed ($\nu = \nu_1$).

The bending moments are as follows

$$\begin{aligned}M_r(r) &= \int_{-h/2}^{h/2} z \sigma_r(r, \zeta) dz = \\ &- \frac{E_1 h^3}{1-\nu^2} \left\{ C_{ww} \left(\frac{d^2 w}{dr^2} + \nu \frac{dw}{rdr} \right) - C_{w\psi} \left(\frac{d\psi}{dr} + \nu \frac{\psi(r)}{r} \right) \right\} \quad (10)\end{aligned}$$

$$\begin{aligned}M_\varphi(r) &= \int_{-h/2}^{h/2} z \sigma_\varphi(r, \zeta) dz = \\ &- \frac{E_1 h^3}{1-\nu^2} \left\{ C_{ww} \left(\frac{dw}{rdr} + \nu \frac{d^2 w}{dr^2} \right) - C_{w\psi} \left(\frac{\psi(r)}{r} + \nu \frac{d\psi}{dr} \right) \right\} \quad (11)\end{aligned}$$

where

$$C_{ww} = \int_{-1/2}^{1/2} \zeta^2 f_e(\zeta) d\zeta, \quad C_{w\psi} = \int_{-1/2}^{1/2} \zeta f_d(\zeta) f_e(\zeta) d\zeta.$$

The equation of equilibrium of the circular plate sector, based on the monograph Timoshenko and Woinowsky-Krieger (1959), is in the following form

$$\frac{d}{dr} [r M_r(r)] - M_\varphi(r) = -r Q(r) \quad (12)$$

where the transverse force of the circular plate subjected to concentrated load (Fig. 1) is as follows

$$Q(r) = \frac{F}{2\pi r} \quad (13)$$

Therefore, the equation of equilibrium (12) with consideration of the expressions (10), (11) and (13) and after simple transformation takes the following form

$$\frac{d}{dr} \left[\frac{1}{r} \frac{d}{dr} \left(C_{ww} r \frac{dw}{dr} - C_{w\psi} r \psi(r) \right) \right] = \frac{1-\nu^2}{2\pi} \frac{1}{r} \frac{F}{E_1 h^3} \quad (14)$$

The elastic strain energy of the plate

$$\begin{aligned}U_\varepsilon &= \pi h \int_{R_0-1/2}^{R_1+1/2} \int [\sigma_r(r, \zeta) \varepsilon_r(r, \zeta) + \sigma_\varphi(r, \zeta) \varepsilon_\varphi(r, \zeta) + \\ &\quad \tau_{rz}(r, \zeta) \gamma_{rz}(r, \zeta)] r d\zeta dr \quad (15)\end{aligned}$$

The work of the load

$$W = -2\pi \int_{R_0}^{R_1} r Q(r) \frac{dw}{dr} dr. \quad (16)$$

Consequently, based on the principle of stationary total potential energy $\delta(U_\varepsilon - W) = 0$, the system of two differential equations of equilibrium of the circular plate is obtained in the following form

$$\begin{aligned}\frac{d}{dr} \left[r \frac{d}{dr} \left(\frac{1}{r} \frac{d}{dr} \left(C_{ww} r \frac{dw}{dr} - C_{w\psi} r \psi(r) \right) \right) \right] = \\ \frac{1-\nu^2}{E_1 h^3} \frac{d}{dr} [r Q(r)] \quad (17)\end{aligned}$$

$$\begin{aligned}\frac{d}{dr} \left\{ \frac{1}{r} \frac{d}{dr} \left(C_{w\psi} r \frac{dw}{dr} - C_{\psi\psi} r \psi(r) \right) \right\} + \\ \frac{1}{2} (1-\nu) C_{\psi\psi} \frac{\psi(r)}{h^2} = 0 \quad (18)\end{aligned}$$

where

$$C_{\psi\psi} = \int_{-1/2}^{1/2} f_d^2(\zeta) f_e(\zeta) d\zeta, \quad C_\psi = \int_{-1/2}^{1/2} \left(\frac{df_d}{d\zeta} \right)^2 f_e(\zeta) d\zeta.$$

It may be easily noticed, that the Eq. (14) is equivalent to the Eq. (17). Therefore, the system of Eqs. (14) and (18) is a basis for analysis of the axisymmetric bending problem of the circular plate with consideration of the shear effect.

3. Bending of the circular plate – analytical studies

The plate is subjected to the concentrated force F (Fig. 1). Integrating the Eq. (14) one obtains

$$C_{ww} \frac{dw}{dr} - C_{w\psi} \psi(r) = \frac{1-\nu^2}{4\pi} \left(2 \frac{C_2}{rR_1} + C_1 \frac{r}{R_1} - \frac{1}{2} \frac{r}{R_1} + \frac{r}{R_1} \ln \frac{r}{R_1} \right) \frac{FR_1}{E_1 h^3} \quad (19)$$

where: C_1, C_2 – integration constants.

The radial displacements for $r=R_0$ are zero, therefore $dw/dr|_{R_0}=0$ and $\psi(R_0)=0$, and from which

$$2C_2 = \left[\frac{1}{2} \left(1 - 2 \ln \frac{R_0}{R_1} \right) - C_1 \right] R_0^2 \quad (20)$$

The form of the right-hand side of the Eq. (19) allows to adopt the following assumptions

$$\frac{dw}{dr} = \frac{1-\nu^2}{4\pi} \frac{w_a}{R_1} \left(2 \frac{C_2}{rR_1} + C_1 \frac{r}{R_1} - \frac{1}{2} \frac{r}{R_1} + \frac{r}{R_1} \ln \frac{r}{R_1} \right) \frac{FR_1}{E_1 h^3} \quad (21)$$

$$\psi(r) = \frac{1-\nu^2}{4\pi} \psi_a \left(2 \frac{C_2}{rR_1} + C_1 \frac{r}{R_1} - \frac{1}{2} \frac{r}{R_1} + \frac{r}{R_1} \ln \frac{r}{R_1} \right) \frac{FR_1}{E_1 h^3} \quad (22)$$

where: w_a, ψ_a coefficients of the deflection $w(r)$ and displacement $\psi(r)$ functions.

The radial bending moment (10) for the simply supported edge is zero ($M_r(R_1)=0$), from which

$$C_1 = -\frac{1-\nu}{2} \cdot \frac{1-(1-2 \ln \alpha_0) \alpha_0^2}{1+\nu+(1-\nu) \alpha_0^2}, \quad (23)$$

where: $\alpha_0=R_0/R_1$ – parameter.

In result the expression (20) is as follows $2C_2 = \tilde{C}_2 \alpha_0^2 R_1^2$, where

$$\tilde{C}_2 = \frac{1-(1+\nu) \ln \alpha_0}{1+\nu+(1-\nu) \alpha_0^2} \quad (24)$$

Taking into account the expressions (21) and (22) based on the Eq. (19) one obtains the algebraic equation

$$C_{ww} \frac{w_a}{R_1} - C_{w\psi} \psi_a = 1 \quad (25)$$

Substituting the expressions (21) and (22) into the Eq. (18) and making use of the Galerkin method one obtains the algebraic equation

$$C_{w\psi} J_1 - \left[C_{\psi\psi} J_1 + \frac{1-\nu}{4} C_{\psi} J_2 \left(\frac{R_1}{h} \right)^2 \right] \psi_a = 0 \quad (26)$$

where:

$$\begin{aligned} J_1 &= \frac{1}{2} \left[(1-C_1)(1-\alpha_0^2) + (1+2\tilde{C}_2) \alpha_0^2 \ln \alpha_0 \right], \\ J_2 &= \frac{1}{32} \left[J_{21}(1-\alpha_0^2) - 4J_{22} \alpha_0^4 \ln \alpha_0 \right], \\ J_{21} &= (8C_1^2 - 12C_1 + 5) (1+\alpha_0^2) - 32(1-C_1) \tilde{C}_2 \alpha_0^2, \\ J_{22} &= 4C_1 + 8\tilde{C}_2 (1+\tilde{C}_2) - 3 + 2 \ln \alpha_0. \end{aligned}$$

The solution of the algebraic Eqs. (25) and (26) gives two unknown coefficients

$$w_a = (1+C_{sc}) \frac{R_1}{C_{ww}}, \quad \psi_a = \frac{C_{w\psi}}{k_{\psi}}, \quad (27)$$

where

$$k_{\psi} = C_{ww} C_{\psi\psi} - C_{w\psi}^2 + \frac{1-\nu}{4} C_{\psi} C_{ww} \frac{J_2}{J_1} \left(\frac{R_1}{h} \right)^2$$

and the dimensionless shear coefficient

$$C_{sc} = \max_{\beta_j} \left(\frac{C_{w\psi}^2}{k_{\psi}} \right) \quad (28)$$

Integrating the expression (21) and taking into account the condition $w(R_1)=0$ (the hinged edge), one obtains the maximum deflection of the circular plate in the following form

$$\begin{aligned} w_{\max}^{(Analyt)} = w(R_0) &= \frac{1-\nu^2}{4\pi C_{ww}} (1+C_{sc}) \times \\ &\times \left[\frac{1}{2} (1-C_1) (1-\alpha_0^2) + \left(\frac{1}{2} + \tilde{C}_2 \right) \alpha_0^2 \ln \alpha_0 \right] \frac{FR_1^2}{E_1 h^3} \end{aligned} \quad (29)$$

After simple transformation of this expression, one obtains

$$w_{\max}^{(Analyt)} = \tilde{w}_{\max}^{(Analyt)} \frac{FR_1^2}{D_1}, \quad (30)$$

where: $D_1 = E_1 h^3 / 12(1-\nu^2)$ – flexural rigidity of the plate, and dimensionless maximum deflection

$$\begin{aligned} \tilde{w}_{\max}^{(Analyt)} &= \frac{1}{48\pi C_{ww}} (1+C_{sc}) \times \\ &\times \left[\frac{1}{2} (1-C_1) (1-\alpha_0^2) + \left(\frac{1}{2} + \tilde{C}_2 \right) \alpha_0^2 \ln \alpha_0 \right] \end{aligned} \quad (31)$$

Moreover, for particular case of the structure – the homogeneous plate ($e_0=1, k_e=1, C_{ww}=1/12$) and $R_0 \rightarrow 0$, the dimensionless maximum deflection (31) with omission of the shear effect ($C_{sc}=0$) is

$$\tilde{w}_{\max}^{(Analyt)} = \frac{3+\nu}{16\pi(1+\nu)}. \quad \text{This}$$

value is consistent with the one presented in the literature, e.g., Timoshenko and Woinowsky-Krieger (1959) and Ventsel and Krauthammer (2001).

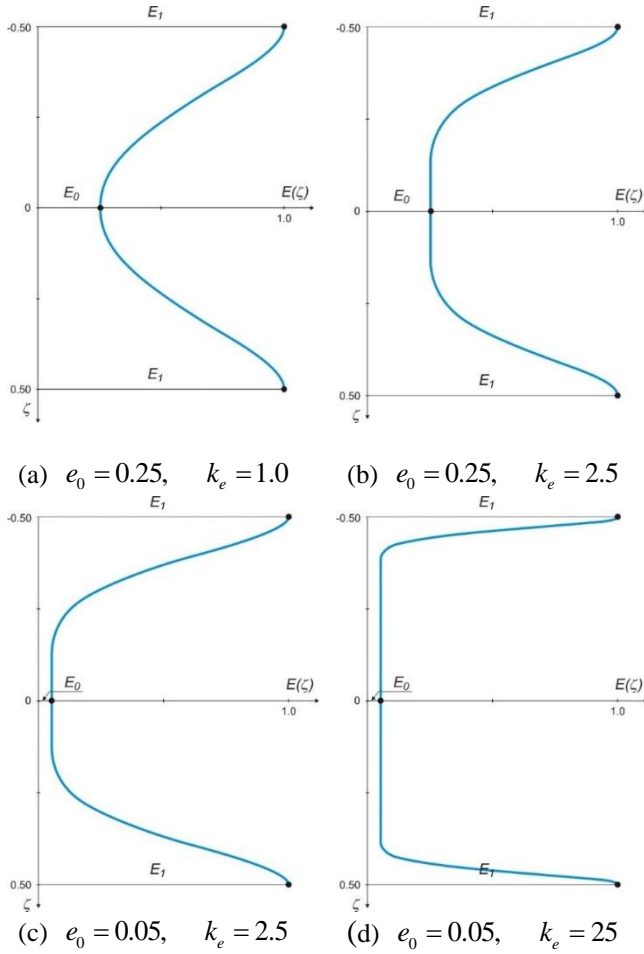


Fig. 3 The graphical illustration of symmetrically varying Young's modulus

Table 1 The results of the calculation of the four exemplary circular plates

e_0	0.25	0.25	0.05	0.05
k_e	1.0	2.5	2.5	25
β_1	1.4079	1.1156	1.5009	0.8841
β_3	-0.6494	0.01337	-0.2459	-0.3041
β_5	0.3208	-0.05984	-0.6210	1.0873
C_{sc}	0.004672	0.004807	0.014988	0.009021
$\tilde{W}_{\max}^{(Analyt)}$	0.05954	0.07094	0.08159	0.19082
$3\beta_1 + 2\beta_3 + \beta_5$	3.246<3.5	3.314<3.5	3.390<3.5	3.131<3.5

The detailed calculations are carried out for the exemplary circular plates. The graphical illustration of the assumed four examples (a, b, c, d) of symmetrically varying mechanical properties is shown in Fig. 3.

The data of the four example plates are as follows: thickness $h=25$ mm, radiuses $R_0=30$ mm, $R_I=600$ mm,

Poisson's ratio $\nu=0.3$. The results of the calculations are specified in Table 1.

It may be noticed that the above four examples of the circular plate are arranged with regard to decreasing rigidity and, in consequence, the values of the maximum deflections $\tilde{W}_{\max}^{(Analyt)}$ grow. The last variant of the plate (Fig. 3(d)) approaches the sandwich structure.

4. Bending of the plate – numerical FEM studies

Numerical computations of the circular plate examples are carried out with the SolidWorks software package. Symmetry of the plate allows to consider the model including only its sector. In this case a quarter of the plate is adopted (Fig. 4), as a sector of the angle smaller than 90° would result in generation of highly deformed finite elements.

The plate models are divided into 3D tetrahedral finite elements with 4 Jacobian points. Example of the mesh is shown in Fig. 5.

The FEM model is computed in linear range, in accordance with the above analytical approach. Several examples of the FEM mesh with various element sizes have shown that the mesh finally adopted is sufficiently fine.

The plate is located in a cylindrical coordinate system. Its origin is placed in the middle of the plate, the longitudinal axis z is perpendicular to the plate and downward directed.

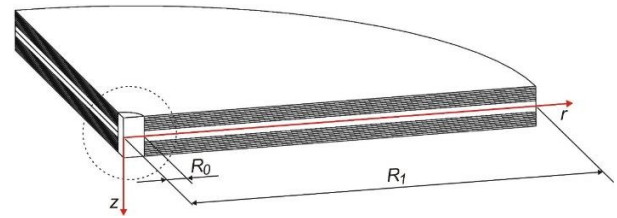


Fig. 4 Exemplary model of the circular plate used for FEM computation

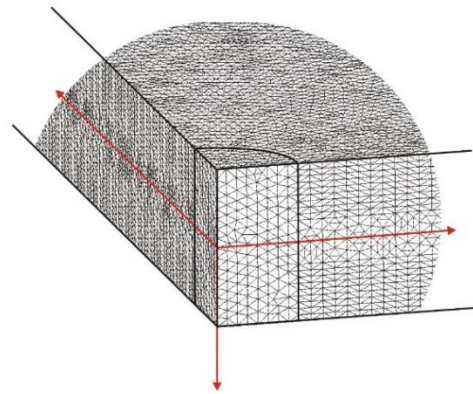


Fig. 5 A part of a FEM mesh (the area marked in Fig. 4 with the dotted circle)

Table 2 The results of numerical FEM calculation of dimensionless deflection in four exemplary cases of the circular plates

e_0	0.25	0.25	0.05	0.05
k_e	1.0	2.5	2.5	25
$\tilde{w}_{\max}^{(FEM)}$	0.06002	0.07123	0.08363	0.18983
$\left \frac{\tilde{w}_{\max}^{(FEM)} - \tilde{w}_{\max}^{(Analyt)}}{\tilde{w}_{\max}^{(FEM)}} \right $	0.8 %	0.4 %	2.5 %	0.5 %

The plate models are composed of several layers of various thicknesses and various Young's moduli, with a view to approximate the Young's modulus patterns shown in Fig. 3. The following boundary conditions imposed at the surfaces of the plate ensure its proper behaviour:

- the plate is simply supported at its edge being a circular circumference of the plate, where the z displacements are zero (the edge is invisible in Fig. 4).
- displacements perpendicular to both vertical cross sections of the plate, being the boundaries of the plate sector, are zeroed due to symmetry of the structure.

The numerical FEM calculation was carried out for the plates of the dimension $R_0=30$ mm and $R_I=600$ mm, loaded with the force $F=20$ kN. The deflections have been converted to their dimensionless values in order to compare the results with those obtained analytically.

Table 2 includes maximum dimensionless deflections so calculated.

Comparison of the above deflection values to those obtained analytically and specified in Table 1 shows excellent convergence of both series of the results.

5. Conclusions

The analytical model of the considered plate takes into account the following:

- the original hypothesis – theory of deformation of the straight line normal to middle surface of the plate (Fig. 2);
- variability of the mechanical properties in the plate thickness direction, expressed by (1) allows to adjust the structures from the homogeneous to sandwich ones.

It allows to describe satisfactorily the shear effect arising in the plate subjected to concentrated load imposed in its centre. In consequence, the deflections are calculated analytically with consideration of the shear effect (demonstrated by the shear coefficient C_{sc} (28)). The numerical model is formulated with the use of 3D tetrahedral finite elements that also take the shear effect into account. Comparison of the analytical and numerical results indicates that the assumed hypothesis – theory efficiently

describes the conditions arising in a real circular plate subjected to the above mentioned load.

References

- Beni, N.N and Dehkordi, M.B. (2018), "An extension of Carrera unified formulation in polar coordinate for analysis of circular sandwich plate with FGM core using GDQ method", *Comp. Struct.*, **185**, 41-434. <https://doi.org/10.1016/j.compstruct.2017.11.044>.
- Debowski D., Magnucki K. and Malinowski M. (2010), „Dynamic stability of a metal foam rectangular plate”, *Steel Compos. Struct.*, **10**(2), 151-168. <https://doi.org/10.12989/scs.2010.10.2.151>.
- Ferreira, A.J.M., Roque, C.M.C. and Martins, P.A.L.S. (2003), "Analysis of composite plates using higher-order shear deformation theory and a finite point formulation based on the multiquadric radial basis function method", *Comp. Part B Eng.*, **34**(7), 627-636. [https://doi.org/10.1016/S1359-8368\(03\)00083-0](https://doi.org/10.1016/S1359-8368(03)00083-0).
- Feyzi, M.R. and Khorshidvand, A.R. (2017), "Axisymmetric post-buckling behavior of saturated porous circular plates", *Thin-Walled Struct.*, **112**, 149-158. <https://doi.org/10.1016/j.tws.2016.11.026>.
- Gunes, R. and Aydin, M. (2010), "Elastic response of functionally graded circular plates under a drop-weight", *Compos. Struct.*, **92**(10), 2445-2456. <https://doi.org/10.1016/j.compstruct.2010.02.015>.
- Jabbari, M., Mojahedin, A., Khorshidvand, A.R. and Eslami, M.R. (2014), "Buckling analysis of a functionally graded thin circular plate made of saturated porous materials", *J. Eng. Mech. - ASCE*, **140**(2), 287-295. [https://doi.org/10.1061/\(ASCE\)EM.1943-7889.0000663](https://doi.org/10.1061/(ASCE)EM.1943-7889.0000663).
- Jha, D.K., Kant, T. and Singh, R.K. (2013), "A critical review of recent research on functionally graded plates", *Compos. Struct.*, **96**, 833-849. <https://doi.org/10.1016/j.compstruct.2012.09.001>.
- Krivoshapko, S.N. (2007), "Research on general and axisymmetric ellipsoidal shells used as domes, Pressure vessels and tanks", *Appl. Mech. Rev.*, **60**(6), 336-355. <https://doi.org/10.1115/1.2806278>.
- Magnucka-Blandzi, E. (2008), "Axi-symmetrical deflection and buckling of circular porous-cellular plate", *Thin-Wall. Struct.*, **46**(3), 333-337. <https://doi.org/10.1016/j.tws.2007.06.006>.
- Magnucka-Blandzi, E., Wisniewska-Mleczko, K. and Smyczynski, M.J. (2018), "Buckling of symmetrical circular sandwich plates with variable mechanical properties of the core in the radial direction", *Compos. Struct.*, **204**, 88-94. <https://doi.org/10.1016/j.compstruct.2018.07.020>.
- Magnucki, K. (2018), "Elastic buckling of a cylindrical panel with symmetrically varying mechanical properties – analytical study", *Compos. Struct.*, **204**, 217-222. <https://doi.org/10.1016/j.compstruct.2018.07.073>.
- Magnucki, K. and Lewinski, J. (2019), "Bending of beams with symmetrically varying mechanical properties under generalized load – shear effect", *Eng. Trans.*, **67**(3), 441-457. <https://doi.org/10.24423/EngTrans.987.20190509>.
- Magnucki, K., Szyk, W. and Lewinski, J. (2002), "Minimization of stress concentration factor in cylindrical pressure vessels with ellipsoidal heads", *Int. J. Press. Vessel Pip.*, **79**(12), 841-846. [https://doi.org/10.1016/S0308-0161\(02\)00101-1](https://doi.org/10.1016/S0308-0161(02)00101-1).
- Magnucki, K., Witkowski, D. and Magnucka-Blandzi, E. (2019), "Buckling and free vibrations of rectangular plates with symmetrically varying mechanical properties – Analytical and FEM studies", *Compos. Struct.*, **220**, 355-361. <https://doi.org/10.1016/j.compstruct.2019.03.082>.

- Maturi, D.A., Ferreira, A.J.M., Zenkour, A.M. and Mashat, D.S. (2014), "Analysis of sandwich plates with a new layerwise formulation", *Compos. Part B Eng.*, **56**, 484-489. <https://doi.org/10.1016/j.compositesb.2013.08.086>.
- Mojahedin, A., Jabbari, M., Khorshidvand, A.R. and Eslami, M.R. (2016), "Buckling analysis of functionally graded circular plates made of saturated porous materials based on higher order shear deformation theory", *Thin-Wall. Struct.*, **99**, 83-90. <https://doi.org/10.1016/j.tws.2015.11.008>.
- Reddy, J.N. (2010), "Nonlocal nonlinear formulations for bending of classical and shear deformation theories of beams and plates", *Int. J. Eng. Sci.*, **48**(11), 1507-1518. <https://doi.org/10.1016/j.ijengsci.2010.09.020>.
- Reddy, J.N. and Berry, J. (2012), "Nonlinear theories of axisymmetric bending of functionally graded circular plates with modified couple stress", *Compos. Struct.*, **94**(12), 3664-3668. <https://doi.org/10.1016/j.compstruct.2012.04.019>.
- Sahraee, S. and Saidi, A.R. (2009), "Axisymmetric bending analysis of thick functionally graded circular plates using fourth-order shear deformation theory", *Europ. J. Mech. – A/Solids*, **28**(5), 974-984. <https://doi.org/10.1016/j.euromechsol.2009.03.009>.
- Saidi, A.R., Rasouli, A. and Sahraee, S. (2009), "Axisymmetric bending and buckling analysis of thick functionally graded circular plates using unconstrained third-order shear deformation plate theory", *Compos. Struct.*, **89**(1), 110-119. <https://doi.org/10.1016/j.compstruct.2008.07.003>.
- Shen, H.S. (2009), *Functionally Graded Materials nonlinear analysis of plates and shells*, CRC Press, Boca Raton, London, New York, USA.
- Sowinski, K. and Magnucki, K. (2018), "Shaping of dished heads of the cylindrical pressure vessel for diminishing of the edge effect", *Thin-Wall. Struct.*, **131**, 746-754. <https://doi.org/10.1016/j.tws.2018.07.018>.
- Timoshenko, S. and Woinowsky-Krieger, S. (1959), *Theory of plates and shells*, (Second Edition), McGraw-Hill Book Company, Inc., New York, Toronto, London.
- Ventsel, E. and Krauthammer, T. (2001), *Thin plates and shells. Theory, analysis, and applications*, Marcel Dekker Inc., New York, Basel, USA.
- Wu, C.-P. and Liu, Y.-C. (2016), "A state space meshless method for the 3D analysis of FGM axisymmetric circular plates", *Steel Comp. Struct.*, **22**(1), 161-182. <https://doi.org/10.12989/scs.2016.22.1.161>.
- Wu, C.P. and Yu, L.T. (2018), "Quasi-3D static analysis of two-directional functionally graded circular plates", *Steel Compos. Struct.*, **27**(6), 89-801. <https://doi.org/10.12989/scs.2018.27.6.789>.
- Yun, W., Rongqiao, X. and Haojiang, D. (2010), "Three-dimensional solution of axisymmetric bending of functionally graded circular plates", *Compos. Struct.*, **92**(7), 1683-1693. <https://doi.org/10.1016/j.compstruct.2009.12.002>.
- Zenkour, A.M. (2006), "Generalized shear deformation theory for bending analysis of functionally graded plates", *Appl. Math. Model.* **30**(1), 67-84. <https://doi.org/10.1016/j.apm.2005.03.009>.
- Zingoni, A. (2002), "Discontinuity effects at cone-cone axisymmetric shell junctions", *Thin-Wall. Struct.*, **40**(10), 877-891. [https://doi.org/10.1016/S0263-8231\(02\)00022-8](https://doi.org/10.1016/S0263-8231(02)00022-8).
- Zingoni, A. (2002), "Parametric stress distribution in shell-of-revolution sludge digesters of parabolic ogival form", *Thin-Wall. Struct.*, **40**(7-8), 691-702. [https://doi.org/10.1016/S0263-8231\(02\)00020-4](https://doi.org/10.1016/S0263-8231(02)00020-4).
- Zingoni, A., Enoma, N. and Govender, N. (2015), "Equatorial bending of an elliptic toroidal shell", *Thin-Wall. Struct.*, **96**, 286-294. <https://doi.org/10.1016/j.tws.2015.08.017>.
- Zingoni, A., Mokhothu, B. and Enoma, N. (2015), "A theoretical formulation for the stress analysis of multi-segmented spherical shells for high-volume liquid containment", *Eng. Struct.*, **87**, 21-31. <https://doi.org/10.1016/j.engstruct.2015.01.002>.

CC